Збірник наукових праць. Серія: Галузеве машинобудування, будівництво

Academic journal. Series: Industrial Machine Building, Civil Engineering

http://journals.pntu.edu.ua/znp
https://doi.org/10.26906/znp.2019.52.1666

UDC 62-932.4

Mathematical modeling for the technological process of surface soil compaction by the inertial vibratory rammer

Ivanchuk Yaroslav[1]*

[1] Vinnytsia National Technical University https://orcid.org/0000-0002-4775-6505
*Corresponding author E-mail: ivanchuck@ukr.net

The high efficiency of the technological process of surface soil compaction using vibration and vibro-impact treatment has been determined. High degree intensification of the soil compaction process is achieved by using original inertial vibratory rammers with a hydro-pulse drive. A new mathematical model has been developed for the surface soil compaction processes study by the inertial vibratory rammers. Using numerical modeling, work dependencies are obtained to determine the main operating characteristics for the technological process of surface soil compaction by inertial vibratory rammers based on a hydro-impulse drive.

Keywords: rammer, compaction, shock, vibration, hydro-impulse drive, inertia, soil, valve.

Математичне моделювання технологічного процесу поверхневого ущільнення ґрунтів інерційною вібротрамбівкою

Іванчук Я.В.[1]*

[1] Вінницький національний технічний університет
*Адреса для листування E-mail: ivanchuck@ukr.net

Визначено високу ефективність технологічного процесу поверхневого ущільнення ґрунтів за допомогою вібраційної і віброударної обробки. Високого ступеню інтенсифікації процесу ущільнення ґрунтів досягнуто застосуванням розроблених оригінальних інерційних вібраційних трамбівок з гідроімпульсним приводом на базі двокаскадного клапана-пульсатора. Розроблено нову математичну модель для дослідження технологічних процесів поверхневого ущільнення ґрунтів інерційною вібротрамбівкою на базі законів гідродинаміки з використанням механореологічної феноменології й узагальнених законів механіки. При розробленні математичної моделі технологічний процес було досліджено на двох фазах: фаза накопичення кінетичної енергії, а також фаза ударної взаємодії інерційної трамбівки з поверхнею ґрунту. На основі розробленої математичної моделі методом кінцевих об'ємів за допомогою чисельного моделювання й методу припасовування отримано розподіл тиску і швидкості робочої рідини в гідроімпульсному приводі інерційної вібротрамбівки. Також було отримано діаграми зміни відносної й абсолютної швидкості рухомих елементів інерційної вібротрамбівки. Розроблена оригінальна модель поверхневого ущільнення ґрунтів дозволила одержати залежності зміни переміщення центрів мас шарів ущільнюючого ґрунту типу суглинків. Одержані робочі залежності основних робочих характеристик інерційної трамбівки на базі гідроімпульсного привода дозволили отримати основні робочі залежності для подальшого підвищення ефективності технологічного процесу поверхневого ущільнення ґрунтів. Отримані результати чисельного моделювання технологічних процесів поверхневого ущільнення ґрунтів інерційною вібротрамбівкою на базі гідроімпульсного привода показали переваги обраного підходу до проектування, а також дозволили довести ефективність розробленої конструкції.

Ключові слова: трамбівка, ущільнення, удар, вібрації, гідроімпульсний привід, інерція, ґрунт, клапан.

Introduction

Technologies characterized by surface treatment processes where pseudo-fluidity of materials is realized [1, 2] with complex rheology and under inertial load conditions, require new developments, study and improvement. Vibrational and vibro-impact technological processes, as well as equipment for their implementation, are widely used [1]. It has been established that if useful vibrations or shock impulses to processing objects are applied, then it can be the flow of a number of technological processes can be significantly intensified, optimal load parameters can be ensured and processing results with high quality parameters can be obtained. In particular, during mechanical surface compaction (ramming), which consists of impacting the load on the soil that falls freely or at a forcibly developed speed, extreme compressive stresses appear in the soil, which cause pseudo-flowability and reorientation of the dispersed soil particles that leads to compaction soil.

Therefore, the study of the changes in the working influence and design parameters of inertial vibratory rammers from a hydro-impulse drive (HID) [1] on the flow of work processes in the surface soil compaction technology increase its effectiveness and outline ways for further development and improvement.

Currently, it is widely used mathematical modeling of workflows in various technological devices. With its help, it is possible to deeply and fully investigate the influence of structural and operational factors on the main characteristics of the device and outline specific ways to improve them, while significantly reducing the amount of experimental research.

Review of research sources and publications

In [2, 3], on the basis of experimental studies, it was found that the best compaction of soils is usually achieved at values of amplitude vibration accelerations close to the acceleration of gravity. Under the action of attractive forces, inertial forces and static load axial forces, particles of a dispersed material tend to reorient and more densely fit each other in a given volume, accompanied by the occupation of more stable equilibrium positions. At the same time, the destruction of the initial structural formations of the «arches» and «bridges» types is observed, followed by a uniform conclusion of the particles forming them, which have an increased mobility in the direction of the static load force by reducing the effective coefficients of internal and lateral friction to zero. In [4, 5] there is researched a fluctuation model particle dispersion medium under the action of vibrations. The phenomena of «vibro-boiling» were analyzed, when a particle loses contact with a vibrating working body, and the bonds between particles decrease and are periodically broken. This state is characterized by loosening of the medium and enhanced circulation of the particles that make it up. The disadvantage of these scientific works is the lack of a mathematically-based behavior of dispersed materials under the action of vibration and vibro-impact load.

In the scientific work [6], a systematic approach to the technological process of forming vibration (VM) and vibro-impact machines (VIM) based on the HID was considered. It enabled to develop a mathematical model for its evaluation. Relationships between the parameters of subsystems on the basis of a vibropress equipment with a HID for forming blanks from powder materials are determined. Based on the mathematical model of fuzzy sets was estimated efficiency of the processing facility. But this technique does not enable to investigate the physicomechanical processes occurring directly in the equipment of the VM and VIM on the basis of the HID.

Definition of unsolved aspects of the problem

Study of physico-mechanical processes that occur in the HID based on the calculations of motion's equations and expenses with a computer [6]. This method does not enable to evaluate the influence of hydrodynamic processes occurring in the executive and regulating units of the HID, despite the complexity of the calculations and the assumptions made in the mathematical description of the working process, which, as experimental data accumulate, can be refined.

Solving these problems is impossible without using the Navier-Stokes equation, which requires the use of the finite volume method to study the complex motion of the working fluid under different flow conditions [5]. Conducting such studies is based on modern methods of mathematical modeling with calculations on a computer using modern, advanced algorithms. It enables to prevent an unjustifiably large number of complex and expensive experimental studies, significantly reduce the time and cost of design work, conduct qualitative and quantitative assessments of physical phenomena with sufficient accuracy for engineering practice [1].

Therefore, the construction of a mathematical model that enables to describe the behavior of a dispersed medium under vibration and vibro-impact load under various operating modes of a HID on the inertial vibratory rammer with the aim of determining the basic performance characteristics of technological processing of building materials is an urgent task.

Problem statement

The aim of the work is to increase the efficiency of theoretical research of the surface soil treatment technology through the development of promising mathematical models for the physical processes of inertial vibration compaction using HID-based devices.

To achieve this goal the following tasks were solved:

– to develop an effective inertial inertial vibratory rammer with HID based on a two-stage pulsator valve. This will allow to realize the most effective modes of vibration impact on the processed media.

– develop the mathematical model for the technology of surface compaction of soils with inertial vibratory rammer based on the HID with a two-stage pulsator valve;

– on the basis of the developed mathematical model, to obtain working dependencies to determine the main characteristics of the studied technological process.

Basic material and results

In Vinnytsia National Technical University, the Department of Industrial Engineering has developed inertial vibratory rammer based on the HID [7]. Figure 1 shows the three-dimensional CAD-model of inertial vibratory rammer based on the HID.

This installation consists of the following main structural elements: to tamping plate 1, through the outer walls 2, attached to the cover 3. The cover 3 is attached to the tamping plate 1 guides 4.

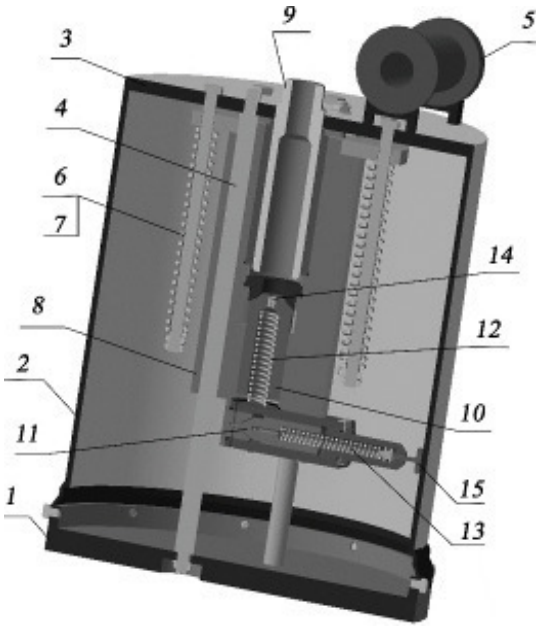

Figure 1 – Three-dimensional model of inertial vibratory rammer based on the HID

In turn, a fastening assembly 5 and a body of a two-stage pulsator valve 8 connected through a power springs 6 and power rails 7 are attached to the cover 3. The housing of the two-stage valve-pulsator 8 additionally performs the functions of a movable hydraulic cylinder in a fixed piston-guide 9. In the case of a two-stage pulsation valve 8 there is a valve of the second cascade 10 and a valve of the first cascade 11. Their mutual movement is regulated by springs 12 and 13, respectively, by the throttle 14 and the adjusting screw 15.

Figure 2 shows the three-component (flat multi-mass) inertial model with irresistible contacts between the masses. It enables to simulate the elastic-viscous properties of soil layers 1, 2, 3 along the x and y axes (the nature of the medium movement along the x and z axes is equivalent, therefore it is advisable to consider only the motion along the x, y axes).

Studies [8] show that oscillations from the working body 4 (see Fig. 2) (ramming plate 1 (see Fig. 1)) inertial vibratory rammer with a mass M are transmitted to the upper layer of soil 1 touching it, with a concentrated mass m_1, and further below are located layers of soil 2, 3, with concentrated masses m_2, m_3. The frequency of oscillations of the entire mass of the soil layer 1 in the zone of vibrations is the same. And the amplitude decreases with distance from the surface of the working body until it goes out altogether.

Thus, a characteristic feature of the operation of inertial vibratory rammers is that the soil is subjected to the vibration effect in a limited area of the working body.

The dimensions of this zone are determined by the oscillation mode and the location of the inertial rammer itself, as well as the properties of the soil itself.

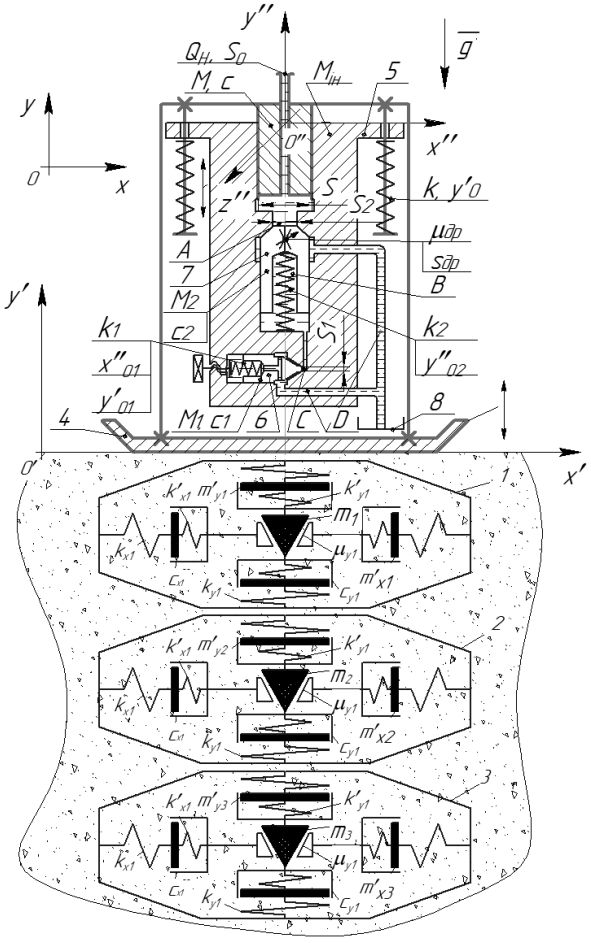

Figure 2 – Dynamic model for the technological process of surface compaction of soil by the inertial vibratory rammer with the HID

There are introduced two moving coordinate systems – $x'O'y'$, rigidly connected to the working body 4, and $x''O''y''$, rigidly connected to the hydraulic cylinder 5 (see Fig. 2) (the body of the two-stage pulsator valve 8 (see Fig. 1)). And also there is introduced the absolute (fixed) coordinate system xOy.

The system of equations (1) for the law of the movement of the soil layers 1, 2, 3 during the contact interaction of the working body 4 with the upper layer of soil 1 is shown in this system of equations:

y_1 – is the absolute coordinate of the working body position4;

y'_1, y'_2, y'_3, x'_1, x'_2, x'_3 – coordinates of the soil masses layers 1, 2, 3;

$k_y = k_{y1}\ k'_{y1} / (k_{y1} + k'_{y1})$, $k_x = k_{x1}\ k'_{x1} / (k_{x1} + k'_{x1})$ – equivalent stiffness of soil layers 1, 2, 3, respectively;

μ_x, μ_y – the projections of the internal friction coefficients on the x and y axes, respectively;

c_{x1}, c_{y1} – component coefficients of viscosity along the x and y axes respectively;

N_{1xy}, N_{2xy}, N_{3xy} – internal reaction forces within the concentrated masses m_1, m_2, m_3 on wedge-shaped platforms at an angle of 45^0;

$m'_{x1} = m'_{y1} = 0$ – additional rheological masses;

$N_{1,4}(t) = k_y y_1' + c_{y1}\dot{y}'_1$ – normal reaction of soil layer 1 to load carrier 4.

$$\begin{cases} -m_1(\ddot{y}_1 + \ddot{y}'_1) = -N_{1,4}(t) + k_y(y'_1 - y'_2)_1 + \\ +c_{y1}(\dot{y}'_1 - \dot{y}'_2) - m_1 g + 2sign(\dot{y}'_1)\mu_y N_{1xy}; \\ -m_2(\ddot{y}_1 + \ddot{y}'_2) = k_y(y'_2 - y'_1) + k_y(y'_2 - y'_3) + \\ +c_{y1}(\dot{y}'_2 - \dot{y}'_1) + c_{y1}(\dot{y}'_2 - \dot{y}'_3) - m_2 g + \\ +2sign(\dot{y}'_2)\mu_y N_{2xy}; \\ -m_3(\ddot{y}_1 + \ddot{y}'_3) = k_y(y'_3 - y'_2) + k_y y'_3 + \\ +c_{y1}(\dot{y}'_3 - \dot{y}'_2) + c_{y1}\dot{y}'_3 - m_3 g + 2sign(\dot{y}'_3)\mu_y N_{3xy}; \\ m_1\ddot{x}'_1 = -k_x x'_1 - c_{x1}x'_1 + sign(\dot{y}'_1)\mu_x N_{1xy}; \\ m_2\ddot{x}'_2 = -k_x x'_2 - c_{x1}x'_2 + sign(\dot{y}'_2)\mu_x N_{2xy}; \\ m_3\ddot{x}'_3 = -k_x x'_3 - c_{x1}x'_3 + sign(\dot{y}'_3)\mu_x N_{3xy}; \\ y'_1 = x'_1;\ y'_2 = x'_2;\ y'_3 = x'_3. \end{cases} \quad (1)$$

The law of the movement for the working body 4:

$$-M\ddot{y} = -Mg + N_{1,4}(t) - \delta k\left(\left(L - y'\right) + y'_0\right) + N_{45}, \quad (2)$$

where M – the mass of the working body 4;

δ – the number of return springs with the rigidity k with the initial tension y'_0;

L – internal height of the inertial ramp;

N_{45} – is the force of the gan working reaction 4 from the contact interaction with the inertia mass 5.

The law of motion for the inertial mass $M_{iн}$ is:

$$-M_{iн}\left(\ddot{y}' + \ddot{y}\right) = -M_{iн}g + \delta k(\left(L - y'\right) + y'_0) - \\ -\iint_{\bar{s}} p_{\bar{s}}(t)dS + c\dot{y}' + N_{2y} + N_{1y} + c_2\dot{y}''_2 - \\ -k_2(|y''|_2 + y''_{02}) - N_{45}, \quad (3)$$

where $p_{\bar{s}}(t)$ – is the changing the pressure function of the working fluid in the internal cavity of a two-stage pulsator valve,

$\iint_{s'} p_{s'}(t)dS$ – forces acting on the inner surface S' of the inertial mass $M_{iн}$,

c_2 – is the coefficient of viscous friction between the walls of the inertial mass 5 and the piston of the working body 4 (see Fig. 2),

N_{2y} –is the vertical component of the reaction force of the conical support from the conical valve of the second stage 7,

N_{1y} – is the vertical component of the reaction force of the cylindrical and conical surfaces valve of the first cascade 6,

c_2 –is the coefficient of viscous friction between the walls of the inertial mass 5 and the valve of the other cascade (see Fig. 2),

k_2 –is the spring stiffness of the valve of the second cascade,

k_2 – is the preload of the valve spring of the second cascade.

Since the valve of the first cascade 6 along the y axis always moves together with the inertial mass 5, it is therefore advisable to record the law of motion of the valve of the first cascade with mass M_1 only for the x axis:

$$-M_1\ddot{x}''_1 = -N_{1x} + k_1(|\ddot{x}_1| + x''_{01}) - \iint_{s'} p_{s'}(t)dS + c_1\dot{x}'', \quad (4)$$

where $p_{s'}(t)$ – the function of pressure change of the working fluid in the internal cavities C and D of the two-stage pulsator valve;

$\iint_{s'} p_{s'}(t)dS$ – forces acting on the inner surface of the inertial mass S';

c_1 – is the coefficient of viscous friction forces between the walls of the inertial mass 5 and the piston of the working body 4 (see Fig. 2);

N_{1x} – is the reaction force of the conical support from the conical valve 7, moreover $N_{1x} = |N_{1y}|$, since the conical surface is made at an angle of 45^0 to the y axis.

The law of movement for the second cascade valve of mass M_2:

$$-M_2(\ddot{y}''_2 + \ddot{y}'' + \ddot{y}) = -M_2 g - \iint_{s''} p_{s''}(t)dS - N_{2y} - \\ -c_2\dot{y}''_2 + k_2(|y''|_2 + y''_{02}), \quad (5)$$

where $p_{s''}(t)$ – is the function of changing the pressure of the working fluid in the internal cavities A and B of the two-stage valve-pulsator;

$\iint_{s''} p_{s''}(t)dS$ – forces acting on the outer surface of the valve of the second cascade S'';

c_2 – is the coefficient of viscous friction forces between the walls of the inertial mass 5 and the piston of the working element 4 (see Fig. 1);

N_{2y} – reaction forces of the conical surface of the valve of the second cascade from the conical seat of the inertia mass 5.

In this case, the inertial forces of the working fluid acting on the operating organs of the inertial vibratory rammer are neglected, as bearing a small contribution to the change in the motion of the inertial vibratory rammer in general.

In order to write down a completely mathematical model of the operation of the inertial vibratory rammer, the operation of the HID at the appropriate working phases of the two-stage valve-pulsator should be considered.

1. Phase of pressure set. In this phase, the conical valves with masses M_1 and M_2 are at rest, and the conical valve M_1 blocks the pressure cavities *A*, *B* and *C* from the drain cavity *D* (see Fig. 1). It leads to a set of pressure in the pressure cavity *A*, so the main pressure $p_s(t)$ acts on the area ($S - S_0$). It should be noted that this phase occurs during the period of time t_1, when the mobile body 4 contacts the surface of the upper soil layer 1. At this phase, the inertial mass $M_{\text{ін}}$. And at this stage there is a joint movement of the inertial mass $M_{\text{ін}}$ and locking elements of mass M_1 and M_2.

For this phase $t_2 \le t \le t_{нт}$ we write the following conditions:

$$\begin{cases} \iint\limits_{s'} p_{s'}(t)dS \le k_1 x''_{01}; \ \iint\limits_{s'} p_{s'}(t)dS < k_2 y''_{01}; \\ y''_2(t) = y''_1(t) = 0; \ \dot{y}''_2(t) = \dot{y}''_1(t) = \dot{y}'(t); \\ x''_1(t) = 0; \ 0 \ge y'_1(t) \ge y'_{1\max}; \ N_{45} = 0, \end{cases} \quad (6)$$

where $y'_{1\max}$ – maximum stroke of inertial mass $M_{ін}$.

2. Phase of operation (opening) of a two-stage pulsator valve. At this phase, the force from the pressure $\iint\limits_{s'} p_{s'}(t)dS$ acting on the area S_1 of the valve of the first cascade 6 is equalized with the tension force of the adjusting spring $k_1 x''_{01}$, that is:

$$\iint\limits_{s'} p_{s'}(t)dS \ge k_1 x''_{01}, \quad (7)$$

leading to open it. When the valve of the first cascade 6 is opened, the pressure cavity *C* communicates with the drain cavity *D*. This cavity message results in the relative velocity of the working fluid in the internal cavity of the two-stage pulsator valve. In turn, the fluid velocity in the internal cavity of a two-stage pulsator valve causes a pressure drop in the pressure cavities *A* and *B* due to the presence of a throttle hole in the valve of the second stage 7. The pressure different in the pressure cavities *A* and *B* results in the appearance of a force cascade move. When it happens, it is in the opening of this valve and, accordingly, the message of the pressure cavity *A* and drain cavity *D*.

At this phase, the inertial mass $M_{\text{ін}}$ also moves to the maximum displacement $y'_{1\max}$, the valve of the first cascade M_1 to the maximum opening $x''_{1\max}$ and the valve of the second cascade M_2 to the maximum opening. Therefore, for this phase $t_{нт} \le t \le t_{сп}$, there are got the following conditions:

$$\begin{cases} \iint\limits_{s'} p_{s'}(t)dS > k_1 x''_{01}; \iint\limits_{s''} p_{s''}(t)dS \ge k_2 y''_{01}; \ y''_1(t) = 0; \\ N_{1x} = 0; \ \dot{y}''_1(t) = \dot{y}'(t); 0 \ge x''_1(t) \ge x''_{1\max}; N_{45} = 0; \\ 0 \ge y''_2(t) \ge y''_{2\max}; N_{2y} = 0; \ 0 \ge y'_1(t) \ge y'_{1\max}. \end{cases} \quad (8)$$

3. Phase closing (lowering) of the two-stage valve-pulsator. At this phase, the working fluid is drained through the drain cavity *D* into the hydraulic tank 8. It causes a pressure drop in the pressure cavities *A*, *B*, *C*. At the same time, the valve of the first cascade with the mass M_1 begins to descend to its original place, (the place of overlap of the pressure cavity *C* from *D*). After the pressure cavity *C* has disconnected from the drain cavity *D*, the relative velocity of the working fluid in the internal cavity of the two-stage pulsator valve becomes zero. In turn, the relative immobility of the working fluid in the internal cavity of a two-stage pulsator valve causes pressure equalization in pressure cavities *A* and *B*. As a result of pressure equalization in pressure cavities *A* and *B*, the spring tension of the second stage valve $k_2(|y''|_2 + y''_{02})$ causes the valve of the second stage 7 to return to its original position. When it occurs, there is the closing of the pressure cavity *A* from the drain cavity *D*.

At this phase, reverse movements of the inertial mass $M_{\text{ін}}$, the valve of the first cascade M_1 and the valve of the second cascade M_2 to the initial position also occur. Therefore, for this phase $t_{сп} \le t \le t_{зк}$, here are the following conditions:

$$\begin{cases} \iint\limits_{s'} p_{s'}(t)dS \ge k_1 x''_{01}; \ \iint\limits_{s''} p_{s''}(t)dS \ge k_2 y''_{01}; \ y''_1(t) = 0; \\ \dot{y}''_1(t) = \dot{y}'(t); \ 0 \ge x''_1(t) \ge x''_{1\max}; \ 0 \ge y''_2(t) \ge y''_{2\max}; \\ 0 \ge y'_1(t) \ge y'_{1\max}; \ N_{45} = 0; N_{2y} = 0; \ N_{1x} = 0. \end{cases} \quad (9)$$

After the end of the closing (lowering) phase of the two-stage pulsator valve, the inertial mass 5 returns to its original position with the acquired speed $\upsilon_{ін} = \dot{y}'_1(t_{зк})$. When this occurs, the impact interaction with the working body 4 occurs. With impact interaction, the inertial mass 5 picks up the working body 4 and they together with the initial velocity υ_M, begin to move upwards (a model of an ordinary body thrown vertically upwards with some initial velocity [9]). The total speed of the entire inertial vibratory rammer υ_M is determined from the law of conservation of momentum [10], namely:

$$\upsilon_M = \frac{\left(M_{in} + M_1 + M_2\right)}{\left(M_{in} + M_1 + M_2 + M\right)}\upsilon_{in}. \quad (10)$$

The movement of the working body 4 should be considered for two cases, namely: when the mobile body 4 contacts the surface of the upper soil layer 1 and when the working body 1 does not contact the surface of the upper soil layer 1 (the jump mode after the shock interaction of the inertial mass 5 and the working body 4).

Conditions working body motion 4 for the jump period

$$t_1 \le t \le t_2 \quad (11)$$

after the shock interaction of the inertial mass 5 and the working body 4 (no contact of the working body 4 with the surface of the topsoil 1) for two cases, namely:

$$\begin{cases} \delta k y_0' > \iint\limits_{\tilde{S}} p_{\tilde{S}}(t)dS;\ y'(t_3) = 0; \\ \dot{y}(t_1) = \upsilon_M;\ \ N_{14}(t) = 0; \end{cases} \quad (12)$$

$$\begin{cases} \delta k y_0' \le \iint\limits_{\tilde{S}} p_{\tilde{S}}(t)dS; \\ N_{14}(t) = 0;\quad N_{45}(t) = 0. \end{cases} \quad (13)$$

Conditions working body motion 4 for the period $t_0 \le t \le t_1$ (t_0 – is the beginning of the countdown of the inertial vibratory ramming operation) of the working body 4 contacting the surface of the topsoil 1. In this case, two cases must also be considered:

$$\begin{cases} t = t;\quad \delta k y' > \iint p\ (t)dS; \\ \dot{y}(t) = -\upsilon;\quad y'(t) = 0, \end{cases} \quad (14)$$

where t_2-t_1=$2\upsilon_M/g$ – flight time inertial vibratory rammer.

To determine the pressure change in the HID cavity, it is necessary to supplement the above laws of motion with the Navier-Stokes system of equations and the continuity equation (15, 16) for weakly squeezed fluids.

In this system of equations (15, 16) $\Omega \in R^3$ – is the three-dimensional region (internal cavity of the HID) in which the working fluid moves, ρ_0 – is the initial density of the working fluid, p_0 – is the initial pressure of the working fluid, Q_H – is the flow rate of the hydraulic pump when fed into the pressure cavity through inlet pipe, S_0 – cross-sectional area of the inlet pipe of the HID.

$$\begin{cases} \frac{1}{\rho}\frac{d\rho}{dt} + \frac{\partial V}{\partial x''} + \frac{\partial V}{\partial y''} + \frac{\partial V}{\partial z''} = 0; \\ \frac{\partial V}{\partial t} + \left(V\frac{\partial V}{\partial x''} + V\frac{\partial V}{\partial y''} + V\frac{\partial V}{\partial z''}\right) = -\frac{1}{\rho}\frac{\partial p}{\partial x''} + \\ + \frac{\nu}{3}\frac{\partial}{\partial x''}\left(\frac{\partial V}{\partial x''} + \frac{\partial V}{\partial y''} + \frac{\partial V}{\partial z''}\right) + \\ + \nu\left(\frac{\partial V}{\partial x''} + \frac{\partial V}{\partial y''} + \frac{\partial V}{\partial z''}\right); \\ \overline{V}\big|_{d\Omega} = 0;\ \Omega \in R^3; \\ \overline{V}\big|_{t=0,z''=0,y''=0,x''=0} = Q_H / S_0; \end{cases} \quad (15)$$

$$\begin{cases} \frac{\partial V_y}{\partial t} + \left(V_x\frac{\partial V_y}{\partial x''} + V_y\frac{\partial V_y}{\partial y''} + V_z\frac{\partial V_y}{\partial z''}\right) = -\frac{1}{\rho}\frac{\partial p}{\partial y''} + \\ + \frac{\nu}{3}\frac{\partial}{\partial y''}\left(\frac{\partial V_x}{\partial x''} + \frac{\partial V_y}{\partial y''} + \frac{\partial V_z}{\partial z''}\right) + \\ + \nu\left(\frac{\partial^2 V_y}{\partial x''^2} + \frac{\partial^2 V_y}{\partial y''^2} + \frac{\partial^2 V_y}{\partial z''^2}\right); \\ \frac{\partial V_z}{\partial t} + \left(V_x\frac{\partial V_z}{\partial x''} + V_y\frac{\partial V_z}{\partial y''} + V_z\frac{\partial V_z}{\partial z''}\right) = -\frac{1}{\rho}\frac{\partial p}{\partial z''} + \\ + \frac{\nu}{3}\frac{\partial}{\partial z''}\left(\frac{\partial V_x}{\partial x''} + \frac{\partial V_y}{\partial y''} + \frac{\partial V_z}{\partial z''}\right) + \\ + \nu\left(\frac{\partial^2 V_z}{\partial x''^2} + \frac{\partial^2 V_z}{\partial y''^2} + \frac{\partial^2 V_z}{\partial z''^2}\right);\ \rho\big|_{t=0,\Omega} = \rho_0. \\ p\big|_{t=0,\Omega} = p_0 + \left(\frac{(m + m_0 + m_3)g + ky_0'}{\left(S - S_0\right)}\right). \end{cases} \quad (16)$$

A mathematical model of the technological process of surface compaction of inertial vibratory rammer, represented by the systems of equations (1) - (16), was implemented by numerical simulation methods based on the FlowVision [11] and Matlab-Simulink [12] software systems. The simulation results are the pressure distribution in the working cavity of the HID inertial vibratory rammer (Fig. 3).

From Figure 3 it can be seen that the throttle 14 mounted in the valve of the second cascade 10 (see Fig. 1) makes a significant character in the pressure change (2 MPa) in the cavity between the valve of the first 11 and the second 10 cascades (see Fig. 1).

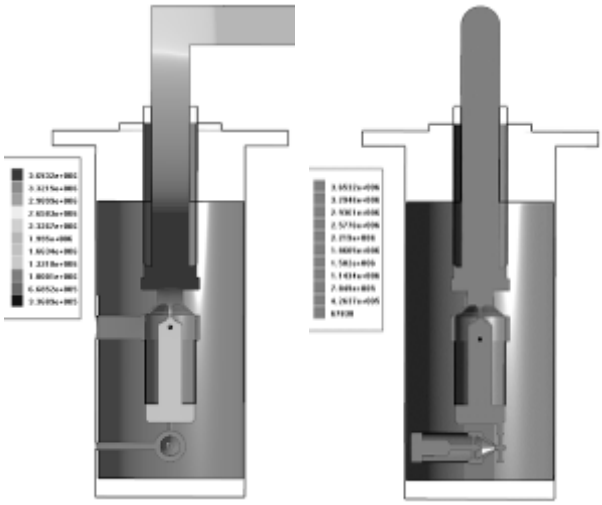

a) b)

Figure 3 – Pressure distribution in the working cavity of inertial vibratory rammer based on the HID:
a) in the *yOz* plane; b) in the *yOx* plane

Also, one of the simulation results is the distribution of pressure and velocity in the working cavity of the HID inertial vibratory rammer (Fig. 4).

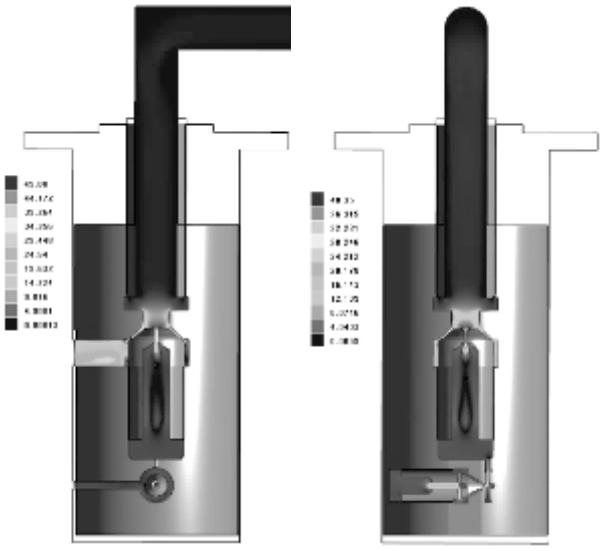

a) b)

Figure 4 – Velocity distribution of the working fluid in the cavity of inertial vibratory rammer based on the HID:
a) in the *yOz* plane; b) in the *yOx* plane

Analyzing Figure 4, it can be observed extreme values of speeds in the valvesseats of the first 11 and second 10 stages, respectively (see Fig. 1), as well as at the throttle bore 14. These extreme speeds can cause cavitation phenomena that can adversely affect technical state of HID parts.

Numerical modeling of hydrodynamic processes of the HID inertial vibratory rammer enabled to obtain:

1) diagrams of pressure changes (Fig. 5) in working cavities *A* and *B* (see Fig. 2);

2) changes in movement (Fig. 6) of the housing of a two-stage pulsator valve 8, valve of the second stage 10 and valve of the first stage 11 relative to tamping plate 1 (see Fig. 1);

3) changes in the speed (Fig. 7) of the housing of the two-stage pulsator valve 8, the valve of the second stage 10 and the relative valve of the first stage 11 relative to the tamping plate 1 (see Fig. 1).

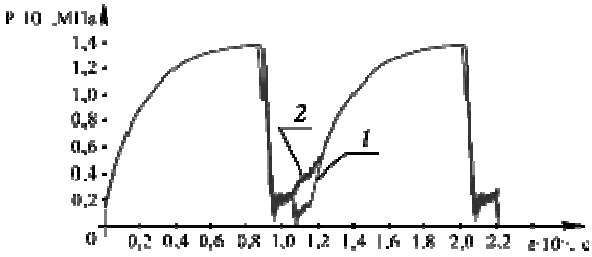

Figure 5 – The pressure distribution of the working fluid in the empty inertial vibrating rammer based on the HID:
1 – in cavity *A*; 2 – in the plane *B*

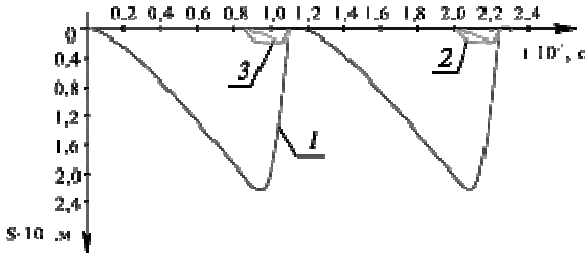

Figure 6 – Changing the movement of moving elements of inertial vibratory rammer based on the HID:
1 – the body of the two-stage valve-pulsator 8;
2 – valve of the second cascade 10;
3 – valve of the first cascade 11

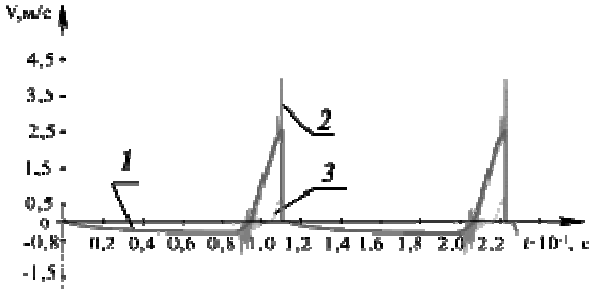

Figure 7 – Changing the speed of moving elements of inertial rammer based on the HID:
1 – the body of the two-stage valve-pulsator 8;
2 – valve of the second cascade 10;
3 – valve of the first cascade 11

Additional absolute displacement diagrams (Fig. 8) of the two-stage pulsator valve 8 body were obtained, taking into account the jump of inertial vibrating rammers over the soil surface 2, as well as the mass' centers of soil layers 1, 2, 3 of the loam type [10] (see Fig. 2).

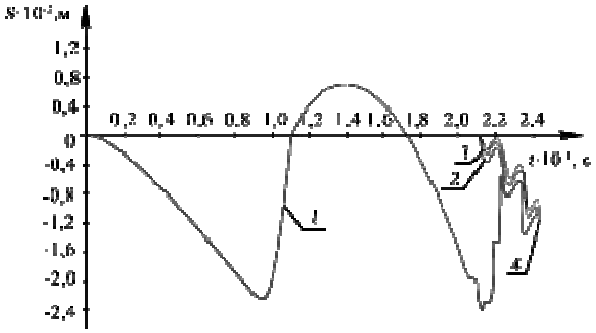

Figure 8 – Change in the absolute movement on technological objects of surface soil compaction:
1 – two-stage valve-pulsator housing;
2 – the mass' center of the soil layer 1;
3 – the mass' center of the soil layer 2;
4 – the mass' center of the soil layer 3

From the absolute displacement diagram for the mass centers of soil layers 1, 2, 3 of the loam type, it can be seen that the maximum deformation of the soil surface (upper layer 1) is 1.2 cm at an oscillation frequency of inertial mass 5 (see Fig. 2) 8.7 Hz.

Conclusions

An effective design of inertial vibrating rammers, based on a two-stage pulsator valve, has been developed. It enables to implement the most effective modes of vibration exposure with surface compaction of the soil.

On the basis of the hydrodynamics laws with the use of mechanical rheological phenomenology and generalized laws of mechanics, a new mathematical model has been developed for the study of technological processes of surface soil compaction with inertial vibratory rammer.

On the basis of the developed mathematical model, using the method of finite volumes using numerical simulation, the working dependences for determining the basic performance characteristics of the technological process of surface soil compaction using inertial vibratory rammer based on the HID are obtained.

The obtained results of numerical simulation for technological processes of surface soil compaction by the inertial vibratory rammer based on the HID. They showed the advantages of the chosen design approach, and also allowed to prove the effectiveness of the developed HID design, based on a two-stage pulsator valve.

References

1. Іскович-Лотоцький, Р.Д., Іванчук, Я.В. (2008). Застосування вібраційного гідроімпульсного привода в будівельних і дорожніх машинах. *Збірник наукових праць Харківської державної академії залізничного транспорту*, 88, 48-54.

2. Wicher, P., Zapletal, F., Lenort, R. & Staš, D. (2016). Measuring the metallurgical supply chain resilience using fuzzy analytic network process. *Journal of Metalurgija*, 55(4), 783-786.

3. Hou, Y.J., Du, M.J., Fang, P. & Zhang, L.P. (2017). Synchronization and stability of an elastically coupled trirotor vibration system. *Journal of theoretical and applied mechanics*. 55(1). 227-240.
http://dx.doi.org/10.15632%2Fjtam-pl.55.1.227

4. Guang, L. & Min, W. (2005). Modeling and controlling of a flexible hydraulic manipulator. *Journal of Central South University of Technology:Science & Technology of Mining and Metallurgy*, 12(5), 578-583.

5. Cheng, C., Chen, H., Shi, Z., Liu, Z. & Xiong, Y. (2016). Modeling and controlling of a flexible hydraulic manipulator. *Journal of Shock and Vibration*, 16, 1–9.

6. Cheng, C., Chen, H., Shi, Z., Liu, Z. & Xiong, Y. (2016). System-level coupled modeling of piezoelectric vibration energy harvesting systems by joint finite element and circuit analysis. *Journal of Shock and Vibration*. 2016, 1-9.
http://dx.doi.org/10.1155/2016/2413578

7. Іскович-Лотоцький. Р.Д., Зелінська. О.В., Іванчук, Я.В. (2018). *Технологія моделювання оцінки параметрів формоутворення заготовок з порошкових матеріалів на вібропресовому обладнанні з гідроімпульсним приводом*. Вінниця: ВНТУ.

8. Jacob, K. (1994). Hurwitz stability of weighted diamond polynomials. *Journal of Systems & Control Letters*, 22(4), 303-312.
https://doi.org/10.1016/0167-6911(94)90062-0

1. Iskovich-Lototsky, R.D. & Ivanchuk, E.V. (2008). Application of vibration hydro-impulse actuator in construction and road machines. *Proceedings of Kharkiv State Academy of Railway Transport*, 88, 48-54.

2. Wicher, P., Zapletal, F., Lenort, R. & Staš, D. (2016). Measuring the metallurgical supply chain resilience using fuzzy analytic network process. *Journal of Metalurgija*, 55(4), 783-786.

3. Hou, Y.J., Du, M.J., Fang, P. & Zhang, L.P. (2017). Synchronization and stability of an elastically coupled trirotor vibration system. *Journal of theoretical and applied mechanics*. 55(1). 227-240.
http://dx.doi.org/10.15632%2Fjtam-pl.55.1.227

4. Guang L. & Min, W. (2005). Modeling and controlling of a flexible hydraulic manipulator. *Journal of Central South University of Technology: Science & Technology of Mining and Metallurgy*, 12(5), 578-583.

5. Cheng, C., Chen, H., Shi, Z., Liu, Z. & Xiong, Y. (2016). Modeling and controlling of a flexible hydraulic manipulator. *Journal of Shock and Vibration*, 16, 1–9.

6. Cheng, C., Chen, H., Shi, Z., Liu, Z. & Xiong, Y. (2016). System-level coupled modeling of piezoelectric vibration energy harvesting systems by joint finite element and circuit analysis. *Journal of Shock and Vibration*. 2016, 1-9.
http://dx.doi.org/10.1155/2016/2413578

7. Iskovich-Lototsky, R.D., Zelinskaya, O.V., Ivanchuk, Y.V. (2018). *Technology of modeling of estimation of parameters of forming of billets from powder materials on the vibropress equipment with the hydropulse actuator. Vinnytsia: VNTU.*

8. Jacob, K. (1994). Hurwitz stability of weighted diamond polynomials. *Journal of Systems & Control Letters*, 22(4), 303-312.
https://doi.org/10.1016/0167-6911(94)90062-0

9. Іскович–Лотоцький, Р.Д., Іванчук, Я.В. (2008). Підвищення ефективності розвантаження матеріалів під дією періодичних ударних імпульсів. *Вібрації в техніці і технологіях*, 2(51), 8-11.

10. Іскович-Лотоцький, Р.Д., Іванчук, Я.В., Веселовський, Я.П. (2016). Оптимізація конструктивних параметрів інерційного вібропрес-молота. *Вісник машинобудування та транспорту*, 2, 43-50.

11. Іскович-Лотоцький. Р.Д., Іванчук, Я.В., Тесовський Д.В.. Веселовський, Я.П. (2012). Застосування гібридного моделювання при розробці установок для утилізації відходів. *Технологічні комплекси,* 1-2 (5-6), 122-126.

12. Wlosnewski, J.C., Kumpugdee-Vollrath, M. & Sriamornsak, P. (2010). Effect of drying technique and disintegrant on physical properties and drug release behavior of microcrystalline cellulose-based pellets prepared by extrusion/spheronization. *Chemical Engineering Research and Design*, 88(1), 100-108.
https://doi.org/10.1016/j.cherd.2009.07.001.

13. Nazarenko, I., Ruchynskyi, M. & Delembovskyi, M. (2018). The basic parameters of vibration settings for sealing horizontal surfaces. *Journal of Engineering and Technology (UAE),* 7 (3.2), 255-259.
http://dx.doi.org/10.14419/ijet.v7i3.2.14415

14. Nesterenko, M., Nazarenko, I. & Molchanov, P. (2018). Cassette installation with active working body in the separating partition. *Journal of Engineering and Technology (UAE)*, 7(3.2), 265-268.
http://dx.doi.org/10.14419/ijet.v7i3.2.14417

15. Nesterenko, M., Maslov, A. & Salenko, J. (2018). Investigation of vibration machine interaction with compacted concrete mixture. *Journal of Engineering and Technology (UAE)*, 7(3.2), 260-264.
http://dx.doi.org/10.14419/ijet.v7i3.2.14416.

9. Iskovich-Lototsky, R.D. & Ivanchuk, Y.V. (2008). Improving the efficiency of unloading materials under the action of periodic shock pulses. *Vibrations in Engineering and Technology,* 2 (51), 8-11.

10. Iskovich-Lototsky, R.D., Ivanchuk, Y.V., Veselovsky, Y.P. (2016). Optimization of design parameters of inertial vibrating press hammer. *Bulletin of Mechanical Engineering and Transport,* 2, 43-50.

11. Iskovich-Lototsky, R.D., Ivanchuk, Y.V., Tesovsky, D.V. & Veselovsky, J.P. (2012). Application of hybrid modeling in the development of waste disposal facilities. *Technological Complexes*, 1-2 (5-6), 122-126.

12. Wlosnewski, J.C., Kumpugdee-Vollrath, M. & Sriamornsak, P. (2010). Effect of drying technique and disintegrant on physical properties and drug release behavior of microcrystalline cellulose-based pellets prepared by extrusion/spheronization. *Chemical Engineering Research and Design*, 88(1), 100-108.
https://doi.org/10.1016/j.cherd.2009.07.001.

13. Nazarenko, I., Ruchynskyi, M. & Delembovskyi, M. (2018). The basic parameters of vibration settings for sealing horizontal surfaces. *Journal of Engineering and Technology (UAE),* 7 (3.2), 255-259.
http://dx.doi.org/10.14419/ijet.v7i3.2.14415

14. Nesterenko, M., Nazarenko, I. & Molchanov, P. (2018). Cassette installation with active working body in the separating partition. *Journal of Engineering and Technology (UAE)*, 7(3.2), 265-268.
http://dx.doi.org/10.14419/ijet.v7i3.2.14417

15. Nesterenko, M., Maslov, A. & Salenko, J. (2018). Investigation of vibration machine interaction with compacted concrete mixture. *Journal of Engineering and Technology (UAE)*, 7(3.2), 260-264.
http://dx.doi.org/10.14419/ijet.v7i3.2.14416.